Citation: CPT Pharmacometrics Syst. Pharmacol. (2019) 8, 177–187; doi:10.1002/psp4.12369

ARTICLE

Target-Mediated Drug Disposition Model for Bispecific Antibodies: Properties, Approximation, and Optimal Dosing Strategy

Johannes Schropp[1,*,†], Antari Khot[2,†], Dhaval K. Shah[2,*] and Gilbert Koch[2,3,*]

Bispecific antibodies (BsAbs) bind to two different targets, and create two binary and one ternary complex (TC). These molecules have shown promise as immuno-oncology drugs, and the TC is considered the pharmacologically active species that drives their pharmacodynamic effect. Here, we have presented a general target-mediated drug disposition (TMDD) model for these BsAbs, which bind to two different targets on different cell membranes. The model includes four different binding events for BsAbs, turnover of the targets, and internalization of the complexes. In addition, a quasi-equilibrium (QE) approximation with decreased number of binding parameters and, if necessary, reduced internalization parameters is presented. The model is further used to investigate the kinetics of BsAb and TC concentrations. Our analysis shows that larger doses of BsAbs may delay the build-up of the TC. Consequently, a method to compute the optimal dosing strategy of BsAbs, which will immediately create and maintain maximal possible TC concentration, is presented.

Study Highlights

WHAT IS THE CURRENT KNOWLEDGE ON THE TOPIC?
☑ Bispecific antibodies (BsAbs) exert their cytotoxic effect by bridging effector T cells and target cells to form immunological ternary complexes (TC) driving the pharmacodynamics. Currently, there are no generalized mathematical models and no quasi-equilibrium (QE) approximation characterizing the relationship between dose and TC formation, which is essential for successful discovery, development, and clinical translation. There is a lack of mathematical framework that can help scientists *a priori* choose an optimal dosing strategy.

WHAT QUESTION DID THIS STUDY ADDRESS?
☑ How to (i) develop the general target-mediated drug disposition model for BsAb, (ii) construct the QE approximation, (iii) characterize the model dynamics, and (iv) compute an optimal dose that immediately creates and maintains maximal possible TC concentrations.

WHAT DOES THIS STUDY ADD TO OUR KNOWLEDGE?
☑ Developed model predicts delayed build-up of TC concentration as the BsAb dose increases. A QE approximation with less parameters was constructed. Optimal working range of the TC is characterized that allows determination of an optimal dosing strategy.

HOW MIGHT THIS CHANGE DRUG DISCOVERY, DEVELOPMENT, AND/OR THERAPEUTICS?
☑ Presented BsAb model can help in optimizing the design of BsAbs and selection of targets. Additionally, the BsAb model/approximation can be used to select an optimal dosing strategy.

Bispecific antibodies (BsAbs) are promising therapeutic modalities that are being developed for different diseases, such as hematologic malignancies, hemophilia, Alzheimer's disease, and Ebola virus.[1–4] Currently, there are two clinically approved BsAbs: blinatumomab for acute lymphoblastic leukemia, and emicizumab for hemophilia A.[2,4] BsAbs induce pharmacological action via various mechanisms, such as bridging effector cells and target cells, modulating a pathway by simultaneously binding to two receptors, or by shuttling the molecule at the site-of-action. These effects are exerted via binding to soluble or membrane bound targets on the same/separate cells.[5,6] Consequently, regardless of

†Shared first authorship. Both authors contributed equally.

[1]Department of Mathematics and Statistics, University of Konstanz, Konstanz, Germany; [2]Department of Pharmaceutical Sciences, School of Pharmacy and Pharmaceutical Sciences, State University of New York at Buffalo, Buffalo, New York, USA; [3]Paediatric Pharmacology and Pharmacometrics Research, University of Basel Children's Hospital (UKBB), Basel, Switzerland. *Correspondence: Johannes Schropp (johannes.schropp@uni-konstanz.de), Dhaval K. Shah (dshah4@buffalo.edu), and Gilbert Koch (gilbert.koch@ukbb.ch)
Received July 16, 2018; accepted October 17, 2018. doi:10.1002/psp4.12369

the mechanism, all BsAbs have potential to exhibit target-driven pharmacokinetics (PKs). Here, we have presented the development of a general target-mediated drug disposition (TMDD) model[7–9] for BsAbs using an immuno-oncology molecule that binds to two different targets present on the membrane of two different cells.

A BsAb that binds to two different targets can form two binary complexes (BCs). Both of these BCs can further bind to the other target to form the ternary complex (TC). This TC is the pharmacologically active species that drives the pharmacodynamic (PD) effect of BsAbs (e.g., designed to redirect T cells toward cancer cells). Thus, TC concentration is pertinent for elucidating PD behavior of BsAbs.[10,11]

Development of a TMDD model for BsAbs is complicated due to the differences in kinetics and binding affinities of both targets. Several models have been developed to describe the PK of BsAbs that bind to cell surface or soluble targets by incorporating target density, turnover rates, affinity, and avidity parameters[12–15] and have been used to characterize plasma and tissue concentrations of BsAbs.[16] However, all these models use parameters that are hard to accurately measure, such as the rapid processes like binding reactions and internalization/degradation of the complexes. Thus, there is need for a reliable approximation of a general BsAb model, which can characterize and predict the kinetics with less number of parameters.

Here, we have presented a general full TMDD model for BsAb. This model is applied to investigate the PK behavior of the TC and to explore an optimal dosing strategy, where optimality is defined by an immediate build-up and maintenance of maximal TC concentration. The model consists of four binding events between six species, leading to the formation of BCs and TCs. It involves target turnover and degradation/internalization of the complexes. To reduce the number of model parameters, the quasi-equilibrium (QE) approximation is constructed based on the fundamental assumption of rapid binding during all four binding events. This approach allows construction of the approximation that retains all model properties available in the full BsAb TMDD model. It is shown that the number of model parameters can be further reduced by assuming that the total receptor concentrations are constant. Furthermore, using the full model and its approximations allow us to reveal important model properties.

We investigated how the changes in target and antibody concentrations affect formation of TC. It is shown that larger doses delay the build-up of the TC, and a method to compute the optimal dosing strategy that immediately creates and maintains the maximal TC concentration is presented. Finally, a simulation-estimation study to address parameter identifiability is included.

METHODS

Theoretical (model structure and equations)

Binding kinetics of the BsAb[12–16] are presented in **Figure 1a**. It is assumed that free BsAb concentration *C binds* to two *targets* (e.g., receptors) R_A and R_B to form BCs, RC_A and RC_B. Both *BCs* further cross-link with the other target creating the TC RC_{AB}. Binding rates k_{onZ} describe the binding of free drug to free receptor or BC, and k_{offZ} describes the dissociation for $Z = 1, \ldots, 4$.

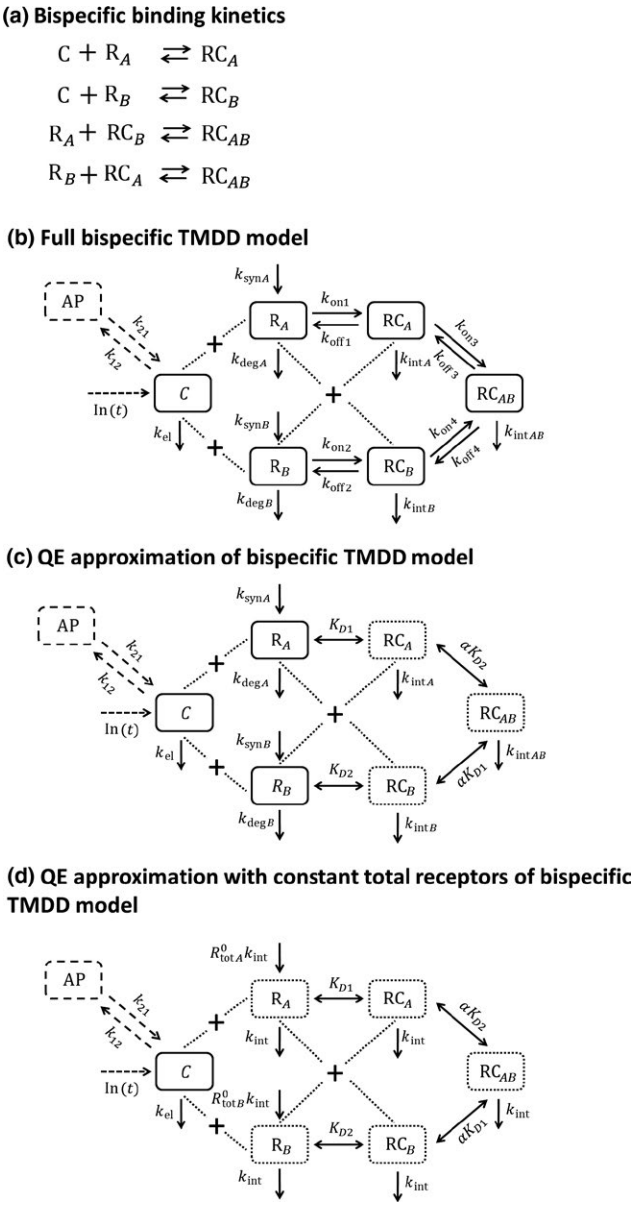

Figure 1 Schematic of bispecific binding kinetics (**a**), full bispecific target-mediated drug disposition (TMDD) model (**b**), quasi-equilibrium (QE) approximation (**c**), and QE approximation with total constant receptors (**d**). Solid boxes reflect the necessity of a differential equation for this state, and the dotted boxes reflect that these states are explicitly available. The peripheral compartment is marked as a dashed box.

We extend the binding kinetics to establish a full BsAb model (**Figure 1b**). Receptors R_A and R_B are generated using zero-order rates k_{synX}, and degraded at first-order rates k_{degX}, where X denotes target A or B. All three formed complexes are assumed to internalize with rates k_{intY}, where Y stands for A, B, or AB. The drug is assumed to eliminate linearly from the central compartment with k_{el}, and distributes to the peripheral compartment AP via k_{12} and k_{21}. Assuming high affinity to the targets and limited capacity of the targets, this model becomes the full BsAb TMDD model.

Table 1 Determinant and entries for the matrix M_{BsAb} (C, R_A, R_B) in Eq. 18 of the quasi-equilibrium approximation

det =	(C*KD2*RA^2 + C^2*KD2*RA + C*KD1*RB^2 + C^2*KD1*RB + C^2*RA*RB + a*KD1^2*KD2^2 + C*KD1*KD2*RA + C*KD1*KD2*RB + KD1*KD2*RA*RB + a*C*KD1*KD2^2 + a*C*KD1^2*KD2 + a*C^2*KD1*KD2 + a*KD1*KD2^2*RA + a*KD1^2*KD2*RB + a*C*KD1*KD2*RA + a*C*KD1*KD2*RB)/(a*KD1^2*KD2^2)
m_{11} =	(C^2*KD2*RA + C^2*KD1*RB + a*KD1^2*KD2^2 + C*KD1*KD2*RA + C*KD1*KD2*RB + a*C*KD1*KD2^2 + a*C*KD1^2*KD2 + a*C^2*KD1*KD2)/(a*KD1^2*KD2^2)
m_{12} =	−(C^2*RA + C*KD1*RB + a*C^2*KD1 + a*C*KD1*KD2)/(a*KD1^2*KD2)
m_{13} =	−(C^2*RB + C*KD2*RA + a*C^2*KD2 + a*C*KD1*KD2)/(a*KD1*KD2^2)
m_{21} =	−(C*RA^2 + KD1*RA*RB + a*C*KD1*RA + a*KD1*KD2*RA)/(a*KD1^2*KD2)
m_{22} =	(C*RA^2 + C*KD1*RA + KD1*RA*RB + a*C*KD1^2 + a*KD1^2*KD2 + a*KD1^2*RB + a*C*KD1*RA + a*KD1*KD2*RA)/(a*KD1^2*KD2)
m_{23} =	−(C*RA − a*C*RA)/(a*KD1*KD2)
m_{31} =	−(C*RB^2 + KD2*RA*RB + a*C*KD2*RB + a*KD1*KD2*RB)/(a*KD1*KD2^2)
m_{32} =	−(C*RB − a*C*RB)/(a*KD1*KD2)
m_{33} =	(C*RB^2 + C*KD2*RB + KD2*RA*RB + a*C*KD2^2 + a*KD1*KD2^2 + a*KD2^2*RA + a*C*KD2*RB + a*KD1*KD2*RB)/(a*KD1*KD2^2)

Parameter α is denoted by *a*.

Models with such detailed mechanisms are usually overparameterized for application and approximations are necessary to reduce the number of parameters. A reasonable approximation reduces complexity of the mechanism but at the same time conserves as many properties of the original model as possible. Under the assumption of high affinity to its targets, rapid binding was assumed for all binding processes to construct the QE approximation (**Figure 1c**). This approximation can be further simplified by assuming either one or both total receptor concentrations are constant (**Figure 1d**), which further reduces the number of parameters.

Finally, properties of the TC are investigated and an optimal dosing strategy to ensure the maximal possible TC concentration is presented.

Full BsAb model. The equations for the full BsAb TMDD model (**Figure 1b**) read:

$$\frac{\mathrm{d}}{\mathrm{d}t}AD = In_{SC}(f,t) - k_a AD \tag{1}$$

$$\frac{\mathrm{d}}{\mathrm{d}t}C = \frac{In_{IV}(t)}{V} + \frac{k_a AD}{V} - k_{el}C - k_{on1}C\cdot R_A + k_{off1}RC_A - k_{on2}C\cdot R_B + k_{off2}RC_B - k_{12}C + k_{21}\frac{AP}{V} \tag{2}$$

$$\frac{\mathrm{d}}{\mathrm{d}t}R_A = k_{synA} - k_{degA}R_A - k_{on1}C\cdot R_A + k_{off1}RC_A - k_{on4}RC_B\cdot R_A + k_{off4}RC_{AB} \tag{3}$$

$$\frac{\mathrm{d}}{\mathrm{d}t}R_B = k_{synB} - k_{degB}R_B - k_{on2}C\cdot R_B + k_{off2}RC_B - k_{on3}RC_A\cdot R_B + k_{off3}RC_{AB} \tag{4}$$

$$\frac{\mathrm{d}}{\mathrm{d}t}RC_A = k_{on1}C\cdot R_A - (k_{off1}+k_{intA})RC_A - k_{on3}RC_A\cdot R_B + k_{off3}RC_{AB} \tag{5}$$

$$\frac{\mathrm{d}}{\mathrm{d}t}RC_B = k_{on2}C\cdot R_B - (k_{off2}+k_{intB})RC_B - k_{on4}RC_B\cdot R_A + k_{off4}RC_{AB} \tag{6}$$

$$\frac{\mathrm{d}}{\mathrm{d}t}RC_{AB} = k_{on4}RC_B\cdot R_A + k_{on3}RC_A\cdot R_B - (k_{off3}+k_{off4}+k_{intAB})RC_{AB} \tag{7}$$

$$\frac{\mathrm{d}}{\mathrm{d}t}AP = k_{12}V\cdot C - k_{21}AP \tag{8}$$

where In_{IV} and In_{SC} are input functions of i.v. and s.c. administration of drug amount, f denotes bioavailability, and V is volume of distribution.

Since BsAbs are engineered molecules, the BsAbs will not be endogenously available prior to treatment. Therefore, existence of an endogenous BsAb baseline was omitted. This implies no or at least negligible endogenous concentration of the mAbs. Consequently, initial values for Eqs. 1–8 are:

$$AD(0)=0,\quad C(0)=0, R_X(0)=\frac{k_{synX}}{k_{degX}}, RC_Y(0)=0 \quad \text{and } AP(0)=0. \tag{9}$$

The full BsAb model Eqs. 1–9 consists of 19 parameters:

$$\theta=\Big(k_{synA},k_{degA},k_{synB},k_{degB},k_{intA},k_{intB},k_{intAB},k_{on1},k_{off1},\ k_{on2},k_{off2},k_{on3},k_{off3},k_{on4},k_{off4},k_{el},k_{12},k_{21},V\Big) \tag{10}$$

Total BsAb concentration and total receptor variables read:

$$C_{tot} = C + RC_A + RC_B + RC_{AB} \tag{11}$$

$$R_{totA} = R_A + RC_A + RC_{AB} \tag{12}$$

$$R_{totB} = R_B + RC_B + RC_{AB} \tag{13}$$

QE approximation of the BsAb model. Rapid binding for the four binding events is approximated with the QE method,[9,17] which means that rapid binding is described by an infinitely fast binding process resulting in a binding equilibrium. Binding rates k_{onZ} and k_{offZ} are substituted by their equilibrium (dissociation) constant:

$$K_{DZ} = \frac{k_{offZ}}{k_{onZ}}$$

According to the principle of microscopic reversibility,[18] in a cyclic reaction mechanism, the individual reactions must balance itself in equilibrium condition by enforcing:

$$K_{D1}K_{D3} = K_{D2}K_{D4} \tag{14}$$

This is equivalent to $K_{D3} = \alpha K_{D2}$ and $K_{D4} = \alpha K_{D1}$, where α denotes the affinity between C and RC_B for R_A, or C and RC_A for R_B. Thus, rapid binding is completely described by only three parameters K_{D1}, K_{D2}, and α.

The QE approximation reads:

$$\frac{\mathrm{d}}{\mathrm{d}t}AD = In_{SC}(f,t) - k_a AD \tag{15}$$

$$\begin{pmatrix} \frac{\mathrm{d}}{\mathrm{d}t}C \\ \frac{\mathrm{d}}{\mathrm{d}t}R_A \\ \frac{\mathrm{d}}{\mathrm{d}t}R_B \end{pmatrix} = M_{BsAb}(C,R_A,R_B)\cdot g_{BsAb}(AD,C,R_A,R_B,AP) \tag{16}$$

$$\frac{\mathrm{d}}{\mathrm{d}t}AP = k_{12}V\cdot C - k_{21}AP \tag{17}$$

where matrix M_{BsAb} (C, R_A, R_B) is of the form:

$$M_{BsAb}(C,R_A,R_B) = \frac{1}{det}\begin{pmatrix} m_{11} & m_{12} & m_{13} \\ m_{21} & m_{22} & m_{23} \\ m_{31} & m_{32} & m_{33} \end{pmatrix} \tag{18}$$

with the determinant *det*. Entries m_{ij} and determinant *det* are listed in **Table 1**. Vector g_{BsAb} (AD, C, R_A, R_B, AP) reads:

$$g_{BsAb}(AD,C,R_A,R_B,AP) = \begin{pmatrix} \frac{In_{IV}(t)}{V} + \frac{k_a AD}{V} - k_{el}C - k_{intA}\frac{R_A C}{K_{D1}} - k_{intB}\frac{R_B C}{K_{D2}} - k_{intAB}\frac{R_A R_B C}{\alpha K_{D1}K_{D2}} - k_{12}C + k_{21}\frac{AP}{V} \\ k_{synA} - k_{degA}R_A - k_{intA}\frac{R_A C}{K_{D1}} - k_{intAB}\frac{R_A R_B C}{\alpha K_{D1}K_{D2}} \\ k_{synB} - k_{degB}R_B - k_{intB}\frac{R_B C}{K_{D2}} - k_{intAB}\frac{R_A R_B C}{\alpha K_{D1}K_{D2}} \end{pmatrix} \tag{19}$$

Explicit equations for the complexes read:

$$RC_A = \frac{C\cdot R_A}{K_{D1}} \tag{20}$$

$$RC_B = \frac{C\cdot R_B}{K_{D2}} \tag{21}$$

$$RC_{AB} = \frac{C\cdot R_A\cdot R_B}{\alpha K_{D1}K_{D2}} \tag{22}$$

Note, with $K_{D1} = K_{D4}$ and $K_{D2} = K_{D3}$ we have $\alpha = 1$. Initial values for the QE approximation Eqs. 15–19 are equal to those from the full model Eq. 9. The number of parameters reduces to 14:

$$\theta = \left(k_{synA}, k_{degA}, k_{synB}, k_{degB}, k_{intA}, k_{intB}, k_{intAB}, \alpha, K_{D1}, K_{D2}, k_{el}, k_{12}, k_{21}, V\right)$$

Derivation of Eqs. 15–22 is provided in **Supplementary Material S1–S10**.

The applied infinitely fast binding process in the QE approximation splits the i.v. administered drug into the part that is immediately bound in the BCs and TC, and the remaining part that is available as free BsAb concentration. This is reflected by multiplication of the input function $In_{IV}(t)$ with factors depending on free BsAb concentration and free receptors. Additionally, $In_{IV}(t)$ acts on the receptor states (compare matrix multiplication in Eqs. 15–19). An appropriate implementation of the QE approximation for i.v. dosing in standard PK/PD software is presented in the Modeling and Simulation section.

QE and constant total receptor approximation of the BsAb model. Further reduction of parameters is possible with the assumption that total receptor concentrations are constant. The relationship

$$k_{degX} = k_{intX} = k_{intAB} =: k_{int} \tag{23}$$

provides

$$R_{totX} \equiv R^0_{totX} = \frac{k_{synX}}{k_{degX}} \tag{24}$$

for both, the full BsAb model and its QE approximation, $X = A, B$. Implementation of this approximation can be provided in two ways. On one hand, the relationship from Eq. 23 can be used in Eqs. 15–22. On the other hand, an equivalent model can be constructed consisting of one differential equation for free BsAb:

$$\frac{\mathrm{d}}{\mathrm{d}t}C = \frac{m_{11}}{det}\left(\frac{In_{IV}(t)}{V} + \frac{k_a AD}{V} - k_{el}C - k_{int}\frac{R_A C}{K_{D1}} - k_{int}\frac{R_B C}{K_{D2}} - k_{int}\frac{R_A R_B C}{\alpha K_{D1}K_{D2}} - k_{12}C + k_{21}\frac{AP}{V}\right) \tag{25}$$

with the explicit representations

$$R_A = \frac{R^0_{totA}}{1 + \frac{C}{K_{D1}} + \frac{R_B C}{\alpha K_{D1}K_{D2}}} \tag{26}$$

and

$$R_B = \begin{cases} R^0_{totB} & \text{for } C = 0 \\ \frac{\left(-b + \sqrt{b^2 - 4ad}\right)}{2a} & \text{for } C > 0 \end{cases} \tag{27}$$

where

$$a = \left(1 + \frac{C}{K_{D2}}\right)\frac{C}{\alpha K_{D1}K_{D2}} \tag{28}$$

$$b = \frac{C\left(R^0_{totA} - R^0_{totB}\right)}{\alpha K_{D1}K_{D2}} + \left(1 + \frac{C}{K_{D2}}\right)\left(1 + \frac{C}{K_{D1}}\right) \tag{29}$$

$$d = -R^0_{totB}\left(1 + \frac{C}{K_{D1}}\right) \tag{30}$$

along with Eqs. 15 and 17, see **Supplementary Material S1–S10** for derivation. The number of parameters now reduces to 10:

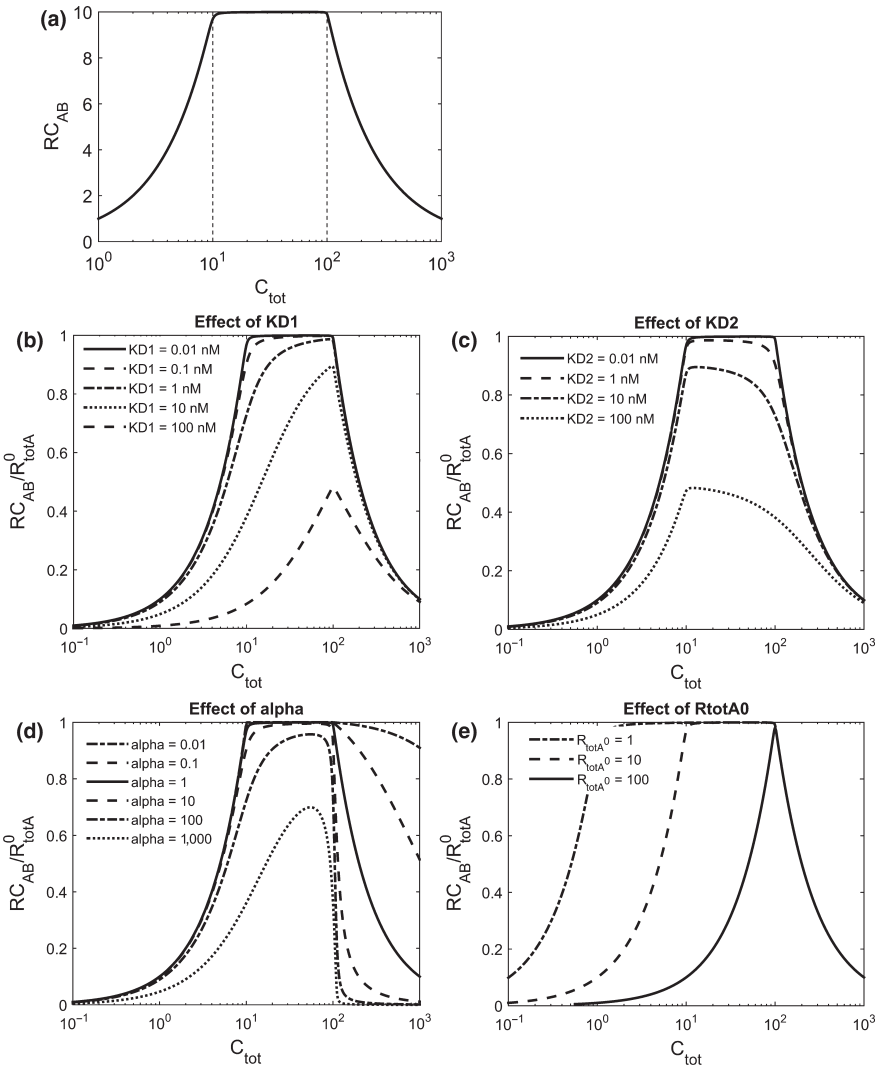

Figure 2 Diagram showing the relationship between total bispecific antibody (BsAb) concentration C_{tot} and the ternary complex RC_{AB} simulated with the equilibrium binding model. (**a**) The typical bell-shaped curve is shown, and the area between the dashed bars shows the optimal working range of the BsAb. Parameter settings are $K_{D1} = K_{D2} = 0.01$ nM, $R^0_{totA} = 10$ nM, $R^0_{totB} = 100$ nM and $\alpha = 1$. To visualize the effect of varying parameter values, only one parameter is changed at a time, over a wide range. Further the *y*-axis was normalized. (**b and c**) The effect of K_{D1} and K_{D2} is shown, (**d**) the effect of α, (**e**) the effect of R^0_{totA}.

$$\theta = \left(R^0_{totA}, R^0_{totB}, k_{int}, \alpha, K_{D1}, K_{D2}, k_{el}, k_{12}, k_{21}, V\right)$$

BsAb concentration-TC relationship. The TC drives the PD effect of BsAbs. Hence, achieving maximal TC concentration will be ideal to observe maximum PD effect.[10,11] To develop an optimal dosing strategy, the BsAb concentration-TC relationship is applied. Li *et al.*[19] developed the equilibrium binding (EB) model, describing pure binding relations, which is the QE model, Eqs. 16, 18–22, completed with

$$0 = k_{degX} = k_{synX} = k_{intX} = k_{el} = k_{12} = k_{21} = k_a, \quad 0 = k_{intY}. \tag{31}$$

This is similar to the closed (*in vitro*) system in case of a standard monoclonal antibody TMDD model[20–22] and can be for the BsAb model equivalently formulated in stationary form by Eqs. 20–22 and 26–30 (see **Supplementary Material S1–S10**).

For any C and any R_{totA} and R_{totB}, the EB model admits an equilibrium description:

$$\left(C, R_A(C), R_B(C), RC_A(C), RC_B(C), RC_{AB}(C)\right) \tag{32}$$

with R_A, R_B according to Eqs. 20–22 and 26–30.

More precisely, we obtain the free BsAb concentration-TC relationship (C, $RC_{AB}(C)$) as:

$$RC_{AB}(C) = \frac{C \cdot R_A(C) \cdot R_B(C)}{\alpha K_{D1} K_{D2}} \tag{33}$$

$$= \frac{RC_A(C) RC_B(C)}{\alpha C} \tag{34}$$

with parameters $\theta = (R_{totA}, R_{totB}, \alpha, K_{D1}, K_{D2})$. Eq. 33 is the equivalent analytical representation of the TC concentration described by Li *et al.*[19] with an implicit system. For low

free BsAb concentrations, TC Eq. 33 increases, whereas in contrast to classical concentration-effect terms,[23,24] TC concentration decreases and finally vanishes for high BsAb concentrations, that is:

$$\lim_{C\to\infty} RC_{AB}(C) = 0 \tag{35}$$

(see **Supplementary Material S1–S10**). This phenomenon is due to the cross-linking reactions. At higher concentrations of BsAb, all receptors are occupied, which interferes in formation of the TC. Hence, RC_A and RC_B saturate at R_{totA} and R_{totB}, and therefore, Eq. 34 enforces Eq. 35.

Structural properties of the TC now become visible, provided the TC concentration is visualized (compare ref. 19) in the total BsAb concentration-TC relationship:

$$(C_{tot}(C), RC_{AB}(C))$$

diagram for fixed given values of R_{totA} and R_{totB}, see **Figure 2a**, in which the typical bell-shaped profile is shown. This diagram suggests an optimal TC concentration, if total BsAb concentration satisfies:

$$\min\left(R_{totA}, R_{totB}\right) \le C_{tot} \le \max\left(R_{totA}, R_{totB}\right). \tag{36}$$

Hence, the relation in Eq. 36 defines the optimal working range of the BsAb.

Optimal dosing strategy for maximal TC concentration. The solutions of the QE approximation and the EB model both satisfy the same algebraic Eqs. 20–22. Thus, any solution of the QE model at an arbitrary time point t_p with $R_{totX}(t_p) = R^0_{totX}$ and $C_{tot}(t_p) = C^0_{tot}$ coincides with the EB model solution Eq. 32 with $C_{tot}(C) = C^0_{tot}$. This allows us to translate dynamical properties from the EB model to the QE approximation and the full model. It means that, in the QE model, the binding parameters characterize the algebraic relationship Eqs. 20–22 and target turnover, elimination and internalization rates determine the values of R_{totX} and C_{tot} or C for which Eq. 32 is evaluated.

Using this relationship between QE and EB model and Eq. 36, an optimal dosing strategy realizing a high TC concentration in the QE approximation must satisfy

$$\min\left(R_{totA}(t), R_{totB}(t)\right) \le C_{tot}(t) \le \max\left(R_{totA}(t), R_{totB}(t)\right) \tag{37}$$

for as many t values as possible.

In case of constant total receptors and $k_{el} = k_{int}$ optimal doses and re-dosing timepoints can be computed explicitly assuring maximal TC concentration. For i.v. bolus administration with no peripheral compartment, we derive (**Supplementary Material S1–S10**):

$$C_{tot}(t) = C^0 \cdot \exp\left(-k_{el} \cdot t\right) \tag{38}$$

where C^0 is the initial free BsAb concentration. Eq. 36 implies $C_{tot}(0) = \max\left(R^0_{totA}, R^0_{totB}\right)$ and we obtain the optimal BsAb amount for the initial dose

$$\text{dose}_{init} = \max\left(R^0_{totA}, R^0_{totB}\right) \cdot V. \tag{39}$$

The re-dosing timepoint is defined by $\min(R^0_{totA}, R^0_{totB}) = C_{tot}(t_{opt})$ and we compute

$$t_{opt} = \frac{1}{k_{el}} \ln\left(\frac{C^0}{\min\left(R_{totA}, R_{totB}\right)}\right). \tag{40}$$

All subsequent doses are

$$\text{dose}_{seq} = \left(\max\left(R^0_{totA}, R^0_{totB}\right) - \min\left(R^0_{totA}, R^0_{totB}\right)\right) \cdot V \tag{41}$$

with multiples of t_{opt} for the re-dosing timepoints.

In general, in full or QE models, the total amount of receptors A and B evolves in time. Nevertheless, an optimal dosing strategy has to generate a total drug concentration satisfying Eq. 37 for as many t values as possible. The optimal initial dose is again given by Eq. 39. However, an optimal re-dosing timepoint cannot be explicitly calculated anymore. But the optimal re-dosing timepoint can be identified when $C_{tot}(t)$ leaves the optimal working range defined by the timepoint t_{opt} satisfying

$$\min\left(R_{totA}(t_{opt}), R_{totB}(t_{opt})\right) = C_{tot}(t_{opt}).$$

All following optimal doses are

$$\text{dose}_{seq} = \left(\max\left(R_{totA}\left(t_{opt}\right), R_{totB}\left(t_{opt}\right)\right) - \min\left(R_{totA}\left(t_{opt}\right), R_{totB}\left(t_{opt}\right)\right)\right) \cdot V.$$

This method allows identification of an optimal dosing strategy for the full model or its QE approximation, provided the model parameter values are known. The basis is the validity of the rapid binding assumption, because singular perturbation theory[25] guarantees that (i) dynamics of the full model and its QE approximation are nearly identical, and (ii) solutions of the QE model in the BCs and TC move along the predictions of the EB model.

Modeling and simulation

Parameter setting for simulations. Applied parameters for pure simulations to reveal profile properties and parameters and results for the simulation-estimation study are presented in **Table 2**. All parameters were roughly based on literature reported values[19,26–28] (conversion factor 1 mg = 6.7 nM). Other applied parameters are mentioned in the text. Typical absolute i.v. bolus doses used are 50 mg and up to 700 mg for s.c. For simulations, a lower limit of quantification (LLOQ) of 0.01 nM was assumed.

Implementation of the QE approximation with an i.v. administration. In the QE approximation, with or without constant total receptors, the i.v. input function $In_{IV}(t)$ is multiplied with different model states and appears at different positions in the equations (compare matrix multiplication in Eqs. 16–19). This affects implementation of i.v. bolus and infusion dosing.

Most standard PK/PD software, such as NONMEM (Icon, Ellicott City, MD) or MONOLIX (Lixoft, Orsay, France), handle drug administration internally with the consequence that the user is not allowed to freely position $In_{IV}(t)$ in the code. More precisely, NONMEM or MONOLIX integrates the ordinary differential equation (ODE) system until the dosing timepoint. In case of i.v. bolus, the dose is added

Table 2 Parameter values for pure simulations (left part) and the simulation-estimation study including results (right part)

Simulation			Simulation-estimation study							
							Final estimates			
							MONOLIX	NONMEM	MONOLIX	NONMEM
Model parameters	Units	Values	Model parameters	Units	True values	Initial estimates	Study 1		Study 2	
V	L	3	k_{el}	1/day	0.1	0.15	0.126	0.118	0.104	0.104
k_a	1/day	0.2	K_{D1}[b]	nM	0.1	0.2	0.1[a]	0.1[a]	0.114	0.13
F	–	0.75	K_{D2}[b]	nM	1	0.5	1[a]	1[a]	1.05	1.04
k_{el}	1/day	0.1	α	–	1[a]	1[a]	1[a]	1[a]	1[a]	1[a]
k_{12}	1/day	0.1	R_A^0	nM	10	15	7.05	8.18	9.78	9.79
k_{21}	1/day	0.03	R_B^0	nM	100	80	78.3	87.5	100	100
k_{on1}	1/(nM day)	10	k_{int}	1/day	0.1	0.1	0.105	0.103	0.100	0.100
k_{off1}	1/day	0.01	V	L	3	2.5	2.73	2.73	2.84	2.85
k_{on2}	1/(nM day)	1	ω_{kel}	–	0.05	1	0.045	0.049	0.023	0.010
k_{off2}	1/day	0.01	ω_V	–	0.05	1	0.058	0.056	0.065	0.066
R_A^0	nM	10	b_1	–	0.2	0.3	0.206	0.205	0.210	0.211
R_B^0	nM	100	b_2	–	0.2	0.3	—	—	0.206	0.206
k_{synA}	nM/day	1	b_3	–	0.2	0.3	—	—	0.207	0.207
k_{degA}	1/day	0.1								
k_{synB}	nM/day	10								
k_{degB}	1/day	0.1								
k_{intA}	1/day	0.05								
k_{intB}	1/day	0.05								
k_{intAB}	1/day	0.1								

[a]Parameter value was fixed during estimation. [b]True values in the full model were (k_{on1}, k_{off1}) = (10,1), (k_{on2}, k_{off2}) = (1,1), (k_{synA}, k_{degA}) = (1,0.1), (k_{synB}, k_{degB}) = (10,0.1) and (k_{intA}, k_{intB}, k_{intAB}) = (0.1,0.1,0.1).
Definitions of all parameters are presented in the text. For simplicity, we assume $k_{on3} = k_{on2}$, $k_{on4} = k_{on1}$, $k_{off3} = k_{off2}$, and $k_{off4} = k_{off1}$. In study 1, data from free bispecific antibody concentration C was refitted. In study 2, data from C and the free receptors R_A and R_B was refitted. Standard deviations of the log-normally distributed interindividual variability are ω_V and ω_{k_a}. Model parameters of the proportional residual error model are b_1, b_2, and b_3. Relative standard errors were all below 5% except for the SDs of the interindividual variability (below 100%) and are, therefore, not reported.

to the drug concentration state and solving the ODE system is continued. In case of i.v. infusion, the infusion rate is added to the right-hand side of the corresponding ODE. These mechanisms can no longer be used for QE/quasi-steady state approximations of more complex models, because $In_{IV}(t)$ is multiplied with different model states and appears at different positions in the equations. Hence, the user has to implement an infusion mechanism. Having this mechanism, an i.v. bolus can be mimicked with a short infusion.

Implementation of an infusion mechanism can be "hard-coded" by hand[17,29]:

```
TDUR = 1e0; duration of infusion, for an i.v. bolus
TDUR
; has to be set very small
IN = 0      ; input function for infusion
; --- Administration of a dose = 335 starting from
; t = 0
IF (T.GE.0. AND T.LE.0+TDUR) THEN
IN = 335*TDUR**(-1)
ENDIF
```

Now $In_{IV}(t)$, described by IN, can be positioned everywhere in the code and multiplied with model states. Dummy timepoints at the start (here $t = 0$) and end of infusion (here $t = t_{dur}$) might be necessary in the dataset for some software to correctly stop and continue integration.

Another possibility is to use a dummy compartment In_{IVDum}

$$\frac{\mathrm{d}}{\mathrm{d}t} In_{\mathrm{IVDum}}(t) = 0 \quad In_{\mathrm{IVDum}}(0) = 0 \tag{42}$$

to mimic the input function $In_{IV}(t)$. With the Tlag and "bioavailability" option, Eq. 42 is controlled with the administrations given in the dataset.

One remark is necessary for an i.v. bolus mimicked by a short i.v. infusion. In case of an i.v. bolus administered drug at $t = 0$, we often also have a measurement at $t = 0$ and, therefore, $C(0) > 0$. In PK/PD software, an i.v. bolus at $t = 0$ is implemented as $C(0) = C_0 + \frac{\mathrm{dose}}{V}$, where $C_0 = 0$ is the initial condition of the free concentration ODE. However, if we mimic i.v. bolus by a short i.v. infusion, we have $C(0) = C^0 = 0$. This may lead to inconsistencies and consequently to numerical difficulties. To overcome this issue, we suggest to slightly shift the measurement in time (e.g., from $t = 0$ to $t = 0.001$).

In case of an absorption compartment, the internal dosing mechanisms from the PK/PD software can be used as usual due to the structure of Eq. 15.

NONMEM and MONOLIX code for the full BsAb model and its approximations with different administrations are available in the **Supplementary Material S1–S10**.

RESULTS

Simulations with the full BsAb model

To visualize the relationship between the BsAbs and the TC, simulations for 50 and 250 mg i.v. doses were performed, using the full model without peripheral compartment. Three properties become visible (**Figure 3**): (i) for the two different doses, area under the curve (AUC) of the BsAb concentration was much larger (400 times in this example) compared to AUC of the TC (1.5 times), (ii) the lower dose causes an immediate build-up of the TC, whereas the higher dose produced a delayed build-up, and (iii) TC formed is much longer available over time for both doses compared to the free BsAb concentration.

To present the behavior of all six components C, R_A, R_B, RC_A, RC_B, and RC_{AB} and to demonstrate the effects of the targets on the free BsAbs concentration profiles, a large i.v. dose of 500, and a large range for free BsAb concentration visualization was used (**Figure 4**). First, a linear elimination followed by a nonlinear elimination phase around $t = 15$ was observed. After an inflection point, these phases are followed again by a linear phase and a nonlinear elimination phase at $t = 55$ followed by a second inflection point. Onsets of recovery of the two targets cause the nonlinear elimination phases and affect the profile of the complexes (**Figure 4**). Effects of varying elimination rate on BsAb concentration and varying internalization rates on all concentration states are shown in **Supplementary Material S1–S10**.

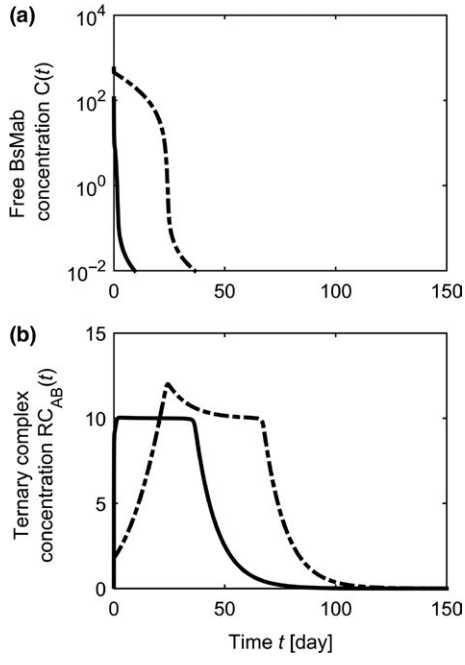

Figure 3 Comparison of the free bispecific antibody (BsAb) concentration C and the ternary complex concentration RC_{AB} simulated with the full model. (**a**) The free BsAb concentration for two different i.v. bolus doses 50 mg (solid line) and 250 mg (dash-dotted line). (**b**) Visualizes the effect on the build-up of the ternary complex.

Comparison of QE approximation with full BsAb model

The approximations assume rapid binding. Therefore, absolute parameter values of k_{onX}, k_{offX} play an essential role. We observed that increasing values for k_{onX}, k_{offX}, but with the same K_{DX}, shifts the full model toward the QE approximation, because the approximation only depends on K_{DX}. Free BsAb profiles using full model and approximation, without peripheral compartment and with i.v. bolus, are

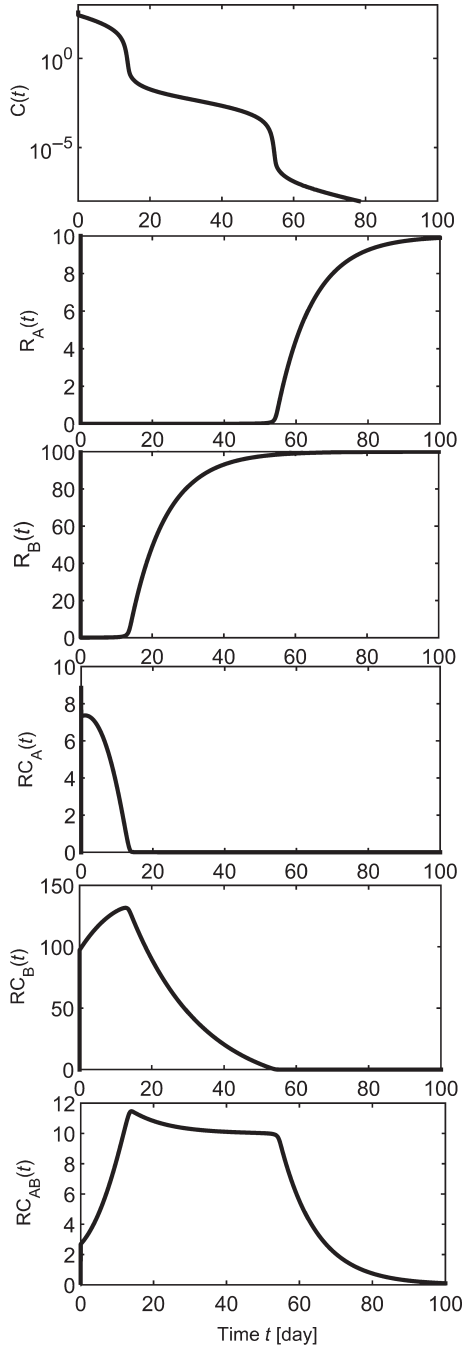

Figure 4 Overall behavior of all six model components C, R_A, R_B, RC_A, RC_B, and RC_{AB} simulated with the full model. The effect of recovery of the free receptors R_A and R_B on the free bispecific antibody concentration C is shown and the relation to the complexes RC_A, RC_B and RC_{AB} can be observed.

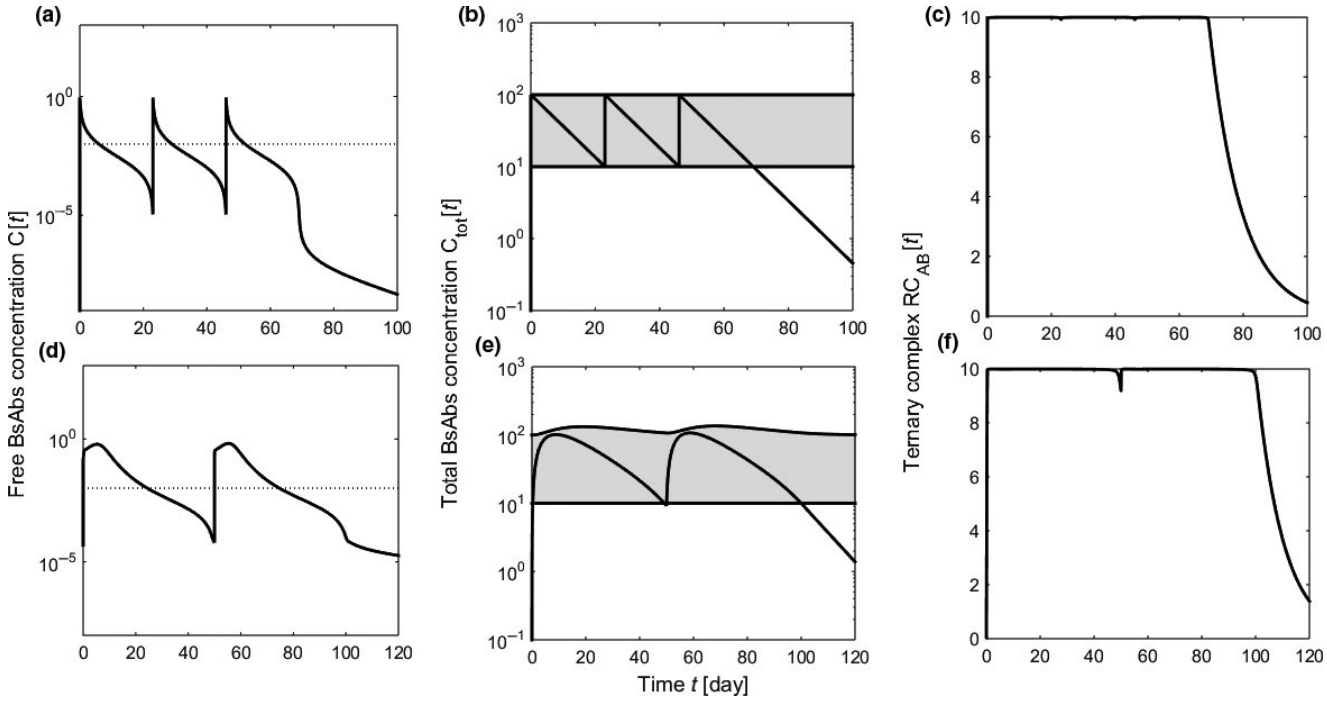

Figure 5 Optimal dosing strategy for i.v. and s.c. administration is visualized. The first example (**a–c**) considers constant total receptors and an i.v. bolus administration. (**a**) Free bispecific antibody (BsAb) concentration is shown after administration of the optimal i.v. bolus dose to keep the total BsAb concentration in the optimal working range (**b**) resulting in the maximal possible concentration of the ternary complex (**c**). Example was produced with the quasi-equilibrium approximation with constant total receptors. The second example (**d–f**) considers nonconstant total receptors and an s.c. administration simulated with the full model.

usually indistinguishable. However, depending on (i) inclusion of a peripheral compartment, (ii) route of administration, and (ii) dose amount, large values of k_{onX}, k_{offX} may be needed. Examples are shown in **Supplementary Material S1–S10**.

Two simulation-estimation studies

In the first study, free BsAb profiles *C* for 30 individuals (12 measurements each over 40 days) were simulated with the full model until LLOQ was reached. In addition, free concentrations of both receptors R_A and R_B (18 measurements each over 70 days) were simulated with the full model until full recovery in the second study. Both datasets were refitted using the QE approximation with constant total receptors. By initial simulations, reasonable initial estimates could be determined for *V*, R_A^0, R_B^0 and partially for k_{el} from *C* profiles, and initial estimates for K_{D1}, K_{D2} from R_A, R_B profiles. Effect of k_{int} was visible in all three profiles. However, α was difficult to obtain from data by visual inspection also due to correlation with K_{D1}, K_{D2}. Fitting of *C* only, resulted in reasonable estimates for *V*, R_A^0, R_B^0, k_{el}, k_{int}. However, K_{D1}, K_{D2} needed to be fixed and were not estimable reflected by convergence problems. Inclusion of R_A, R_B data to fitting, resulted in good final estimates for *V*, R_A^0, R_B^0, k_{el}, k_{int} and, in addition, K_{D1}, K_{D2}, whereas α was partially difficult to estimate and was, therefore, fixed. All parameters (true values, and initial and final estimates) are presented in **Table 2**. Applied source codes for MONOLIX and NONMEM, and visual predictive checks are available in **Supplementary Material S1–S10**. We observed that sometimes representation Eqs. 15, 17, 25–30 caused convergence issues in MONOLIX and, therefore, we suggest using the representation Eqs. 15–23.

Effects of varying binding parameters and total receptor concentration on the TC

TC behavior with respect to total BsAb concentration and total receptor concentrations can be simulated for different binding parameters with the EB model *Eqs* 20–22 and 26–30. In **Figure 2b–e** the effect of varying K_{D1}, K_{D2}, R_{totA}^0,R_{totB}^0, α are shown. The model predicted a decrease in TC concentration, even at significantly higher BsAb concentrations, with lower target affinities (K_{D1}, K_{D2}). Additionally, increase in α also reduced TC concentrations due to increase in dissociation constants. MATLAB code is available to test the effect of different model parameters in **Supplementary Material S1–S10**.

Optimal dosing strategy for maximal TC concentration

First, the QE approximation with constant total receptors, realized with $k_{int} = k_{intA} = k_{intB} = k_{intAB} = 0.1$ is considered. Further we assume $k_{el} = k_{int}$, allowing an explicit computation of the optimal dosing timepoints. For simplicity, the peripheral compartment was neglected. The constant total receptors $R_{totA}^0 \equiv 10\,\text{nM}$, $R_{totB}^0 \equiv 100\,\text{nM}$ define the optimal working range $R_{totA}^0 \le C_{tot}(t) \le R_{totB}^0$ (**Figure 5b**). Hence, the optimal initial dose to achieve $C_{tot}(0) = 100$ is $\text{dose}_{init} = 44.8$ mg, see Eq. 39. All subsequent doses are $\text{dose}_{seq} = 40.3$ mg, see Eq. 41. Optimal re-dosing was $t_{opt} = 23$ day, computed by Eq. 40. Note that (i) $C(0) \approx 1$ due to high affinity, and (ii) *C* is already far below LLOQ at t_{opt}

(**Figure 5a**). Hence, although nearly no free BsAb is available, the system still runs (**Figure 5c**). A re-dose at the time $t = 7$ day, when LLOQ was reached for free BsAb would lead to suboptimal TC concentration.

Second, the full model is considered with peripheral compartment and s.c. administration. Here, no explicit formulas for optimal doses and timepoints can be presented. However, simulations show that an initial dose of $dose_{init} = 100$ mg was sufficient to bring the total drug concentration in the upper limit of the optimal working range (**Figure 5e**). The optimal re-dose timepoint was $t_{opt} = 50$ day with subsequent doses of $dose_{seq} = 100$ mg. Again, free BsAb was below the LLOQ after 25 days but the optimal re-dose timepoint is two times later.

DISCUSSION

We have presented a TMDD model, along with its QE approximation, for BsAbs that are designed to work by forming a TC between two different cell types. The model includes typical antibody and target properties, such as linear elimination, a peripheral compartment, target turnover, and degradation/internalization of the BCs and TC.

The aims were (i) to construct model approximations to reduce the number of parameters, (ii) to reveal model properties that are discernible only in those simplified formulations, (iii) to construct an optimal dosing strategy to immediately build-up and maintain the maximal TC concentration, and (iv) to use the full model and the approximations to investigate the effects of the model parameters on the dynamics.

Under the assumption of high affinity of the BsAb to its targets and limited capacity of the targets, rapid binding is the basic assumption to construct a QE approximation with a reduced number of parameters. Further parameter reduction is possible when either one or both total receptor concentrations are constant over time. We observed that because only the ratio of the binding parameters is used in the QE approximations, the absolute values of the binding parameters with same ratio are important for how the full model moves toward the approximation. Finally, the EB model was constructed (i.e., a QE model without target turnover, and elimination and internalization rates), which characterizes the TC concentration with respect to total BsAb concentration and the total receptors. How to set up a quasi-steady state approximation was not obvious because the principle of microscopic reversibility relies on the dissociation constants and not on the steady state constant. Although, a Michaelis-Menten approximation can be obtained by assuming the typical temporary property of full receptor occupancy, it was not possible to further reduce the number of parameters. As a result of the rapid binding approximation via an infinitely fast process, the matrix notation reveals that the i.v. drug input function is multiplied with different model states and appears at different positions in the model equations. This property was already observed for approximations of less complex TMDD models (e.g., for competitive interaction of endogenous and exogenous antibodies).[17,29] Unfortunately, most internal i.v. administration mechanisms in PK/PD software are not flexible enough to handle this situation. Hence, we demonstrated how an i.v. administration has to be included by the user in the model code of the QE approximation.

A second focus was the design of an optimal dosing strategy for maximal TC concentration. For that, we exploited properties from the EB model with respect to total BsAb concentration-TC relationship. This led to the construction of an optimal working range for BsAbs. In this range, the total BsAb concentration is within the minimum and the maximum of both total receptor concentrations, leading to maximal possible TC concentration. By construction of the EB model, those results can be translated back to the QE approximation and finally under the rapid binding assumption to the full model. Please note that an optimal dosing strategy for patients has to account for intersubject variability in target turnover.

BsAbs are promising candidates for cancer immunotherapy. However, due to the cross-linking structure of the formed complexes, the functional TC of BsAb shows different PK properties compared to classical concentration-effect terms. More precisely, the model predicts a delayed build-up of TC concentration for increasing doses. We have even showed that TC concentration tends to be zero for very high BsAb concentrations. This finding is corroborated by *in vitro* studies, performed by coculturing Jurkat T cells and Daudi B cells in the presence of CD19xCD3 DART, where a decrease in TC concentration was observed at higher concentrations of BsAb.[30] For the development of an efficacious BsAb, a fine balance is required between target kinetics and antibody properties. The presented model was used to analyze the effects of various target and antibody related parameters on the formation of the TC. Due to the cross-linking nature of the binding kinetics, we observed that although the free BsAb concentration can be below the LLOQ, the BsAb mechanism still produces maximal TC concentrations. Using the optimal working range, we showed how optimal re-dosing timepoints and doses can be obtained. Another interesting aspect observed during the analysis was increase in target mediated clearance due to faster internalization of receptor. BsAb exhibit two inflection points in the concentration-time curve, the first point is primarily due to elimination of BC and the second inflection indicates elimination of TC. Faster internalization of target receptors affects the first inflection point leading to faster elimination of BsAb. This inevitably shortens the residence time of BC and TC in the system (**Supplementary Material S1–S10**). Similarly, higher internalization of TC leads to faster elimination of BsAb, evident at the second inflection point (**Supplementary Material S1–S10**). Apart from providing insights into the key target-related parameters that might affect the formation of TC, this model can also aid in predicting PKs of BsAb eliminating at different rates. Currently, there are different BsAb (i.e., full size immunoglobulin G BsAb and $(ScFv)_2$ BsAb), which exhibit clearance in the range of 10^{-5} to 10^{-3} L/hour depending on their size and structure, and this model can provide a quantitative framework for suitable antibody selection and engineering.

In the future, the model and its approximation can be extended with (i) TC effects on target cells,[28] (ii) T cell rebound phenomena,[31] and (iii) integration of local geometrical

structures on the cell surface for the cross-linking binding reactions.[12,13] Inclusion of geometrical structures leads to mathematical models of the form Eqs. 1–8, with binding rates partially depending on the target concentrations. Development of a QE approximation and the design of an optimal dosing strategy for these kinds of models are interesting topics for future research.

Supporting Information. Supplementary information accompanies this paper on the *CPT: Pharmacometrics & Systems Pharmacology* website (www.psp-journal.com).

Supplementary Material S1. Supplemental material for target-mediated drug disposition model for bispecific antibodies: properties, approximation, and optimal dosing strategy.
Supplementary Material S2. Matlab implementation of the model Eqs. 20–22 and 26–30.
Supplementary Material S3. Example code of the quasi-equilibrium approximation with nonconstant total receptors in MONOLIX.
Supplementary Material S4. Example code of the full model in MONOLIX.
Supplementary Material S5. Example code of the quasi-equilibrium approximation with nonconstant total receptors in NONMEM.
Supplementary Material S6. Example code of the full model in NONMEM.
Supplementary Material S7. Applied MONOLIX source code for Eqs. 15–23.
Supplementary Material S8. Alternative MONOLIX source code for Eqs. 15 , 17, and 25–30.
Supplementary Material S9. Applied NONMEM source code for Eqs. 15–23.
Supplementary Material S10. Alternative NONMEM source code for Eqs. 15, 17, and 25–30.

Conflict of Interest. The authors declared no competing interests for this work.

Author Contributions. J.S., A.K., D.K.S., and G.K. wrote the manuscript. J.S., A.K., D.K.S., and G.K. performed the research.

Funding. D.K.S. is supported by National Institutes of Health (NIH) grants GM114179 and AI138195.

1. Hultqvist, G., Syvanen, S., Fang, X.T., Lannfelt, L. & Sehlin, D. Bivalent brain shuttle increases antibody uptake by monovalent binding to the transferrin receptor. *Theranostics* **7**, 308–318 (2017).
2. Oldenburg, J. & Levy, G.G. Emicizumab prophylaxis in hemophilia A with inhibitors. *N. Engl. J. Med.* **377**, 2194–2195 (2017).
3. Wec, A.Z. *et al.* A "Trojan horse" bispecific-antibody strategy for broad protection against ebolaviruses. *Science* **354**, 350–354 (2016).
4. Kantarjian, H. *et al.* Blinatumomab versus chemotherapy for advanced acute lymphoblastic leukemia. *N. Engl. J. Med.* **376**, 836–847 (2017).
5. Yang, F., Wen, W. & Qin, W. Bispecific antibodies as a development platform for new concepts and treatment strategies. *Int. J. Mol. Sci.* **18**, pii: E48 (2016).
6. Trivedi, A. *et al.* Clinical pharmacology and translational aspects of bispecific antibodies. *Clin. Transl. Sci.* **10**, 147–162 (2017).
7. Levy, G. Pharmacologic target-mediated drug disposition. *Clin. Pharmacol. Ther.* **56**, 248–252 (1994).
8. Mager, D.E. & Jusko, W.J. General pharmacokinetic model for drugs exhibiting target-mediated drug disposition. *J. Pharmacokinet. Pharmacodyn.* **28**, 507–532 (2001).
9. Mager, D.E. & Krzyzanski, W. Quasi-equilibrium pharmacokinetic model for drugs exhibiting target-mediated drug disposition. *Pharm. Res.* **22**, 1589–1596 (2005).
10. Barr, I.G., Buchegger, F., MacDonald, H.R., Carrel, S. & von Fliedner, V. Retargeting of cytolytic T lymphocytes by heteroaggregated (bispecific) antibodies. *Cancer Detect. Prev.* **12**, 439–450 (1988).
11. Huehls, A.M., Coupet, T.A. & Sentman, C.L. Bispecific T-cell engagers for cancer immunotherapy. *Immunol. Cell Biol.* **93**, 290–296 (2015).
12. Doldan-Martelli, V., Guantes, R. & Miguez, D. G. A mathematical model for the rational design of chimeric ligands in selective drug therapies. *CPT Pharmacometrics Syst. Pharmacol.* **2**, e26 (2013).
13. Rhoden, J.J., Dyas, G.L. & Wroblewski, V.J. A modeling and experimental investigation of the effects of antigen density, binding affinity, and antigen expression ratio on bispecific antibody binding to cell surface targets. *J. Biol. Chem.* **291**, 11337–11347 (2016).
14. van Steeg, T.J., Bergmann, K.R., Dimasi, N., Sachsenmeier, K.F. & Agoram, B. The application of mathematical modelling to the design of bispecific monoclonal antibodies. *mAbs* **8**, 585–592 (2016).
15. Harms, B. D., Kearns, J. D., Su, S.V., Kohli, N., Nielsen, U.B. & Schoeberl, B. Optimizing properties of antireceptor antibodies using kinetic computational models and experiments. *Methods Enzymol.* **502**, 67–87 (2012).
16. Chudasama, V.L., Zutshi, A., Singh, P., Abraham, A.K., Mager, D.E. & Harrold, J.M. Simulations of site-specific target-mediated pharmacokinetic models for guiding the development of bispecific antibodies. *J. Pharmacokinet. Pharmacodyn.* **42**, 1–18 (2015).
17. Koch, G., Jusko, W.J. & Schropp, J. Target-mediated drug disposition with drug-drug interaction, Part I: single drug case in alternative formulations. *J. Pharmacokinet. Pharmacodyn.* **44**, 17–26 (2017).
18. Colquhoun, D., Dowsland, K.A., Beato, M. & Plested, A.J. How to impose microscopic reversibility in complex reaction mechanisms. *Biophys. J.* **86**, 3510–3518 (2004).
19. Li, L., Gardner, I. & Gill, K. Modeling the binding kinetics of bispecific antibodies under the framework of a minimal human PBPK model. AAPS NBC Poster Number T2056; 2014.
20. Gabrielsson, J., Peletier, L.A. & Hjorth, S. In vivo potency revisited – keep the target in sight. *Pharmacol. Ther.* **184**, 177–188 (2018).
21. Peletier, L.A. & Gabrielsson, J. New equilibrium models of drug-receptor interactions derived from target-mediated drug disposition. *AAPS J.* **20**, 69 (2018).
22. Gabrielsson, J., Peletier, L.A. & Hjorth, S. Lost in translation: what's in an EC50? Innovative PK/PD reasoning in the drug development context. *Eur. J. Pharmacol.* **835**, 154–161 (2018).
23. Goutelle, S. *et al.* The Hill equation: a review of its capabilities in pharmacological modelling. *Fundam. Clin. Pharmacol.* **22**, 633–648 (2008).
24. Koch, G., Schropp, J. & Jusko, W.J. Assessment of non-linear combination effect terms for drug-drug interactions. *J. Pharmacokinet. Pharmacodyn.* **43**, 461–479 (2016).
25. Vasileva, A.B. Asymptotic behaviour of solutions to certain problems involving nonlinear differential equations containing a small parameter multiplying the highest derivatives. *Russian Math. Surv.* **18**, 13–83 (1963).
26. Yoshida, K. *et al.* Two target TMDD model described nonlinear pharmacokinetics of a bispecific antibody for fibroblast growth factor receptor 1/betaKlotho complex in humans. *American Conference on Pharmacometrics* 17 October 2017. Poster T-083.
27. Gibiansky, L. Modeling Drugs with Target-Mediated Disposition. PAGE 2011.
28. Jiang, X. *et al.* Development of a Target cell-Biologics-Effector cell (TBE) complex-based cell killing model to characterize target cell depletion by T cell redirecting bispecific agents. *mAbs* **10**, 876–889 (2018).
29. Koch, G., Jusko, W.J. & Schropp, J. Target mediated drug disposition with drug-drug interaction, part II: competitive and uncompetitive cases. *J. Pharmacokinet. Pharmacodyn.* **44**, 27–42 (2017).
30. Moore, P.A. *et al.* Application of dual affinity retargeting molecules to achieve optimal redirected T-cell killing of B-cell lymphoma. *Blood* **117**, 4542–4551 (2011).
31. Ferl, G.Z. *et al.* A preclinical population pharmacokinetic model for anti-CD20/CD3 T-cell-dependent bispecific antibodies. *Clin. Transl. Sci.* **11**, 296–304 (2018).